

Supporting Information

Origin of Electric Field-dependent Charge Generation in Organic Photovoltaics with Planar and Bulk Heterojunctions

Kyohei Nakano^{a,}, Yumiko Kaji^a, and Keisuke Tajima^{a,*}*

^aRIKEN Center for Emergent Matter Science (CEMS), 2-1 Hirosawa, Wako, Saitama 351-0198,
Japan

Corresponding Author

*Kyohei Nakano: kyohei.nakano@riken.jp; *Keisuke Tajima: keisuke.tajima@riken.jp

Table S1. Summary of the molecular structures and the suppliers for the semiconducting materials used in this study.

Short name	Full name	Supplier, catalog codes	Molecular structure
PM6 (PBDB-T-2F)	Poly[(2,6-(4,8-bis(5-(2-ethylhexyl-3-fluoro)thiophen-2-yl)-benzo[1,2-b:4,5-b']dithiophene))-alt-(5,5-(1',3'-di-2-thienyl-5',7'-bis(2-ethylhexyl)benzo[1',2'-c:4',5'-c']dithiophene-4,8-dione)]	Solarmer, P9203	
PTB7	Poly({4,8-bis[(2-ethylhexyl)oxy]benzo[1,2-b:4,5-b']dithiophene-2,6-diyl} {3-fluoro-2-[(2-ethylhexyl)carbonyl]thieno[3,4-b]thiophenediyl})	1-Material, OS0007	
PTB7-Th (PCE10)	Poly[4,8-bis(5-(2-ethylhexyl)thiophen-2-yl)benzo[1,2-b:4,5-b']dithiophene-2,6-diyl-alt-(4-(2-ethylhexyl)-3-fluorothieno[3,4-b]thiophene-)-2-carboxylate-2,6-diyl]]	1-Material, OS0100	
PFN-Br	Poly(9,9-bis(3'-(N,N-dimethyl)-N-ethylammonium-propyl-2,7-fluorene)-alt-2,7-(9,9-dioctylfluorene))dibromide	Ossila, M2230A3	

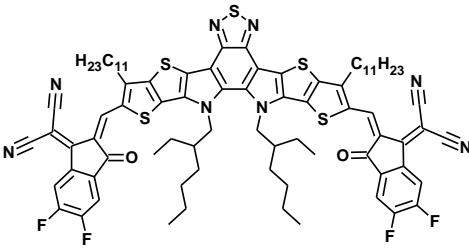
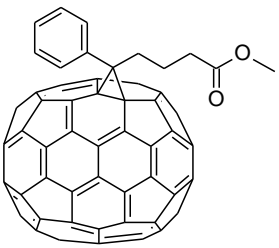
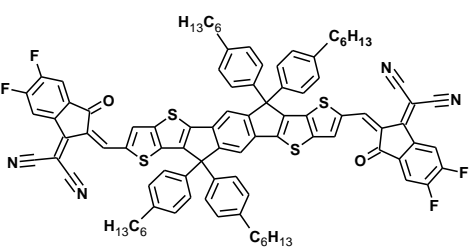
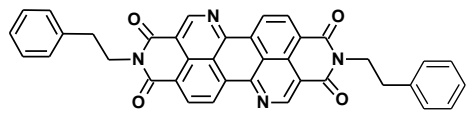
Y6	2,2'-((2Z,2'Z)-((12,13-bis(2-Ethylhexyl)-3,9-diundecyl-12,13-dihydro-[1,2,5]thiadiazolo[3,4-e]thieno[2'',3''':4',5']thieno[2',3':4,5]pyrrolo[3,2-g]thieno[2',3':4,5]thieno[3,2-b]indole-2,10-diyl)bis(methanylylidene))bis(5,6-difluoro-3-oxo-2,3-dihydro-1H-indene-2,1-diylidene))dimalononitrile	Solarmer, N5101	
PC ₇₁ BM	[6,6]-Phenyl C71 butyric acid methyl ester	Solenne	
IT-4F	3,9-Bis(2-methylene-(3-(1,1-dicyanomethylene)-6,7-difluoro)-indanone))-5,5,11,11-tetrakis(4-hexylphenyl)-dithieno[2,3-d:2',3'-d']-s-indaceno[1,2-b:5,6-b']dithiophene	Solarmer, YI428A	
PhC ₂ -BQQDI	-	FUJIFILM Wako, DLN2002	

Table S2. Summary of film preparation conditions. CB: chlorobenzene; CF: chloroform; DIO: 1,8-diodooctane; CN: 1-chloronaphthalene.

OPVs	Structure	Acceptor	Donor
PhC ₂ -BQQDI//PM6	PHJ	Thermally evaporated	8.0 mg/mL in CB, 1000 rpm
PC ₇₁ BM//PM6	PHJ	6.0 mg/mL in CF, 600 rpm	8.0 mg/mL in CB, 1000 rpm
IT-4F//PM6	PHJ	6.0 mg/mL in CF, 600 rpm	8.0 mg/mL in CB, 1000 rpm
Y6//PM6	PHJ	5.0 mg/mL in CF, 600 rpm	8.0 mg/mL in CB, 1000 rpm
Y6//PTB7	PHJ	5.0 mg/mL in CF, 600 rpm	8.0 mg/mL in CB, 1000 rpm
Y6//PTB7-Th	PHJ	5.0 mg/mL in CF, 600 rpm	8.0 mg/mL in CB, 1000 rpm
			Donor:acceptor
PM6:PC ₇₁ BM	BHJ	3.8:5.9 mg/mL in CF + 0.15% DIO, 700 rpm, annealing 110 °C/10 min	
PM6:IT-4F	BHJ	3.7:4.4 mg/mL in CF, 700 rpm, annealing 110 °C/10 min	
PM6:IT-4F(DIO)	BHJ	3.7:4.4 mg/mL in CF + 0.15% DIO, 700 rpm, annealing 110 °C/10 min	
PM6:Y6	BHJ	3.7:4.4 mg/mL in CF + 0.15% CN, 700 rpm, annealing 110 °C/10 min	

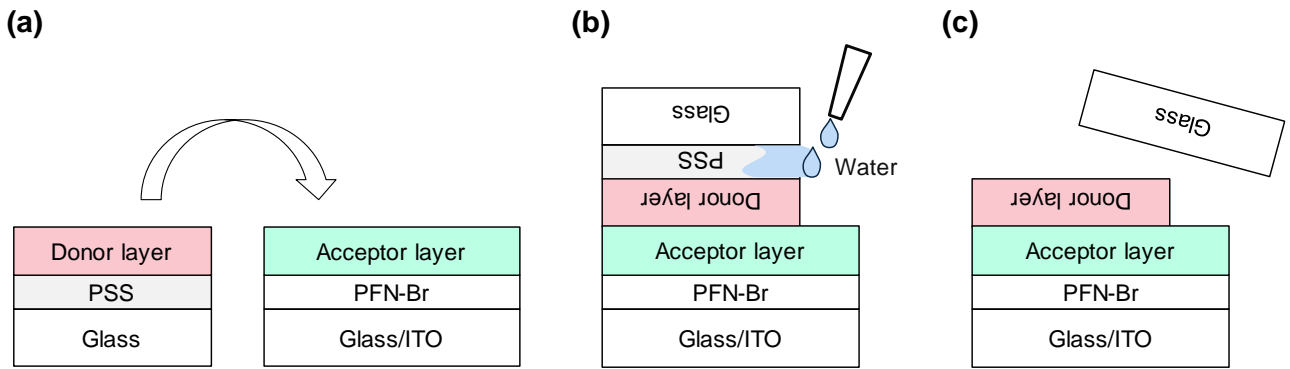


Figure S1 | Schematics of the contact film transfer process for fabricating a PHJ device. (a) Donor and acceptor layers are prepared on different substrates by spin-coating. The donor layer is formed on a glass substrate covered with a poly(4-styrenesulfonic acid) (PSS) layer, which is water soluble. The acceptor layer is formed on an indium tin oxide (ITO) transparent electrode with a buffer layer (PFN-Br). The glass substrate with the donor layer is placed on the acceptor layer so that the donor and acceptor layers are in contact with each other. (b) A small amount of water is dropped on the edge of the substrate and dissolves only the PSS layer. (c) Top glass substrate is detached, and the PHJ structure is obtained without heat or pressure.

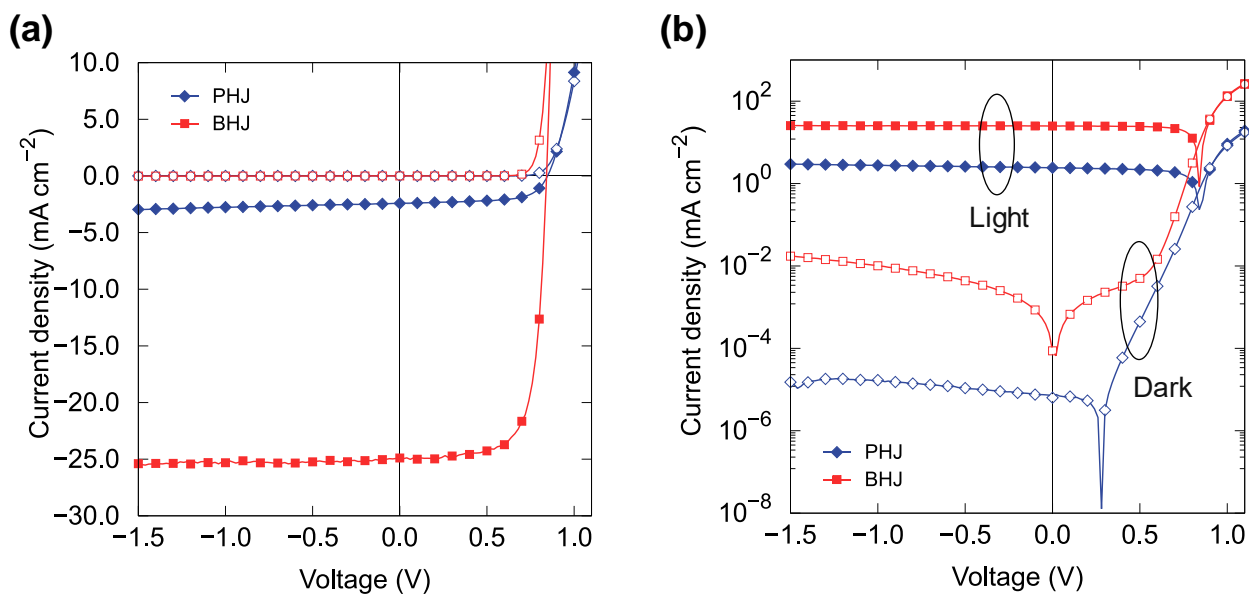


Figure S2 | Comparison of $J-V$ curves of the PHJ and BHJ devices. $J-V$ characteristics under AM1.5 100 mW/cm^2 simulated sunlight irradiation and dark conditions on (a) a linear scale and (b) a semi-logarithmic scale. The current density is nonzero at 0 V in the PHJ device under dark conditions because the measured current is close to the detection limit of the source meter.

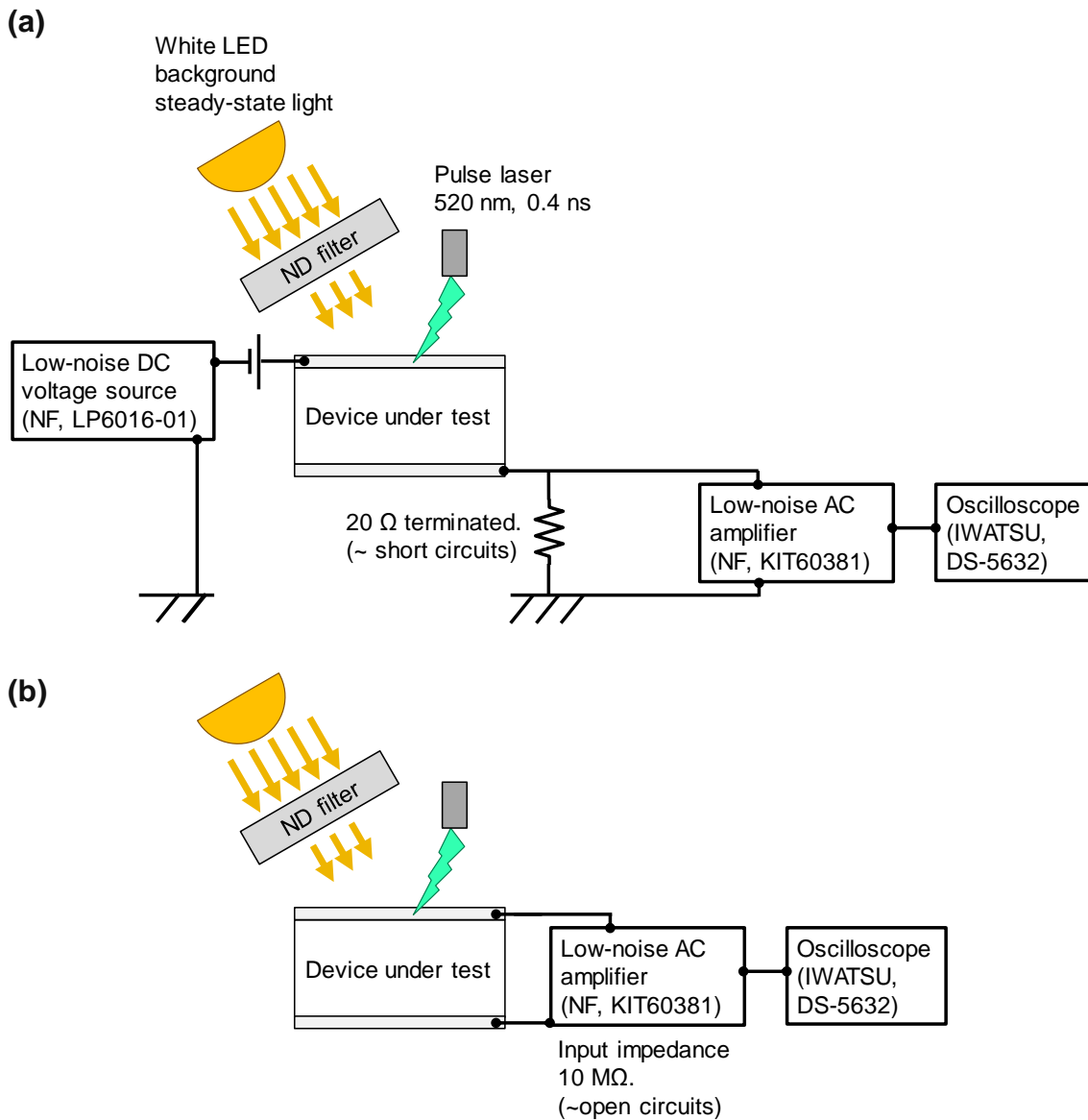


Figure S3 | Experimental setup for (a) transient photocurrent and (b) photovoltage measurements. ND, neutral density.

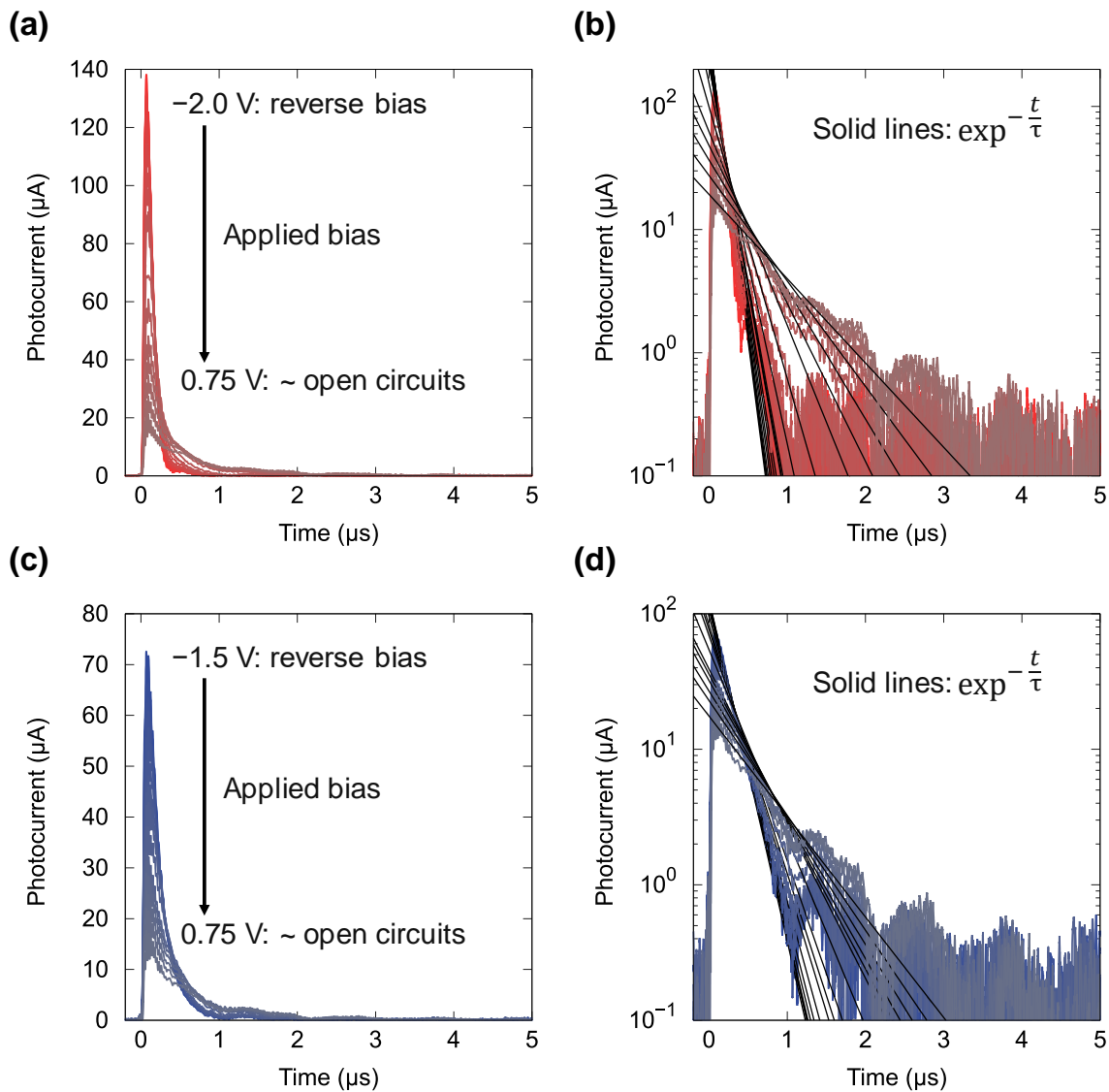


Figure S4 | Raw transient photocurrent signals. Results for the PM6:Y6 BJJ device on (a) a linear and (b) a semi-logarithmic scale. The steady-state background white LED light intensity was 100% (generated the same J_{SC} under AM1.5 100 mW/cm² irradiation). The applied voltage was scanned from -2.0 V (reverse bias) to 0.75 V (near open circuit conditions). The exponential function was fitted to the initial signal decay, and extraction time τ was obtained. The solid lines in (b) are the fitting results. (c), (d) Transient photocurrent results for the Y6/PM6 PHJ device.

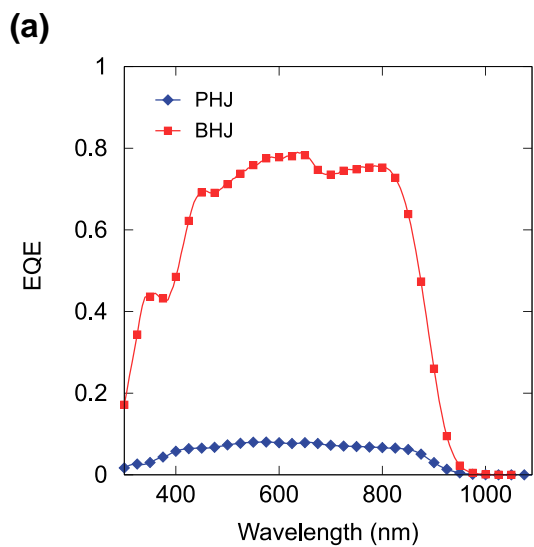


Figure S5 | (a) EQE spectra of PHJ and BHJ devices using a PM6 donor and Y6 acceptor.

Supplementary Note S1| Effect of buffer layers and interlayers on the field-dependent charge generation

To discuss the effect of the buffer layers on the charge generation process, we fabricated a three-layered structure by film transfer twice, in which the PM6:Y6 BHJ film was inserted between the Y6 and PM6 planar heterojunctions (PHJs) (Figure S6a). As the thickness of the inserted bulk heterojunction (BHJ) layer increased, J_{SC} increased because of the large donor/acceptor (D/A) interface area in the BHJ layer (Figure S6b). The slope in the J - V curve became small for thick BHJs (Figure S6c), and the 50 nm BHJ layer showed almost electric field-independent charge generation similar to the BHJ device. The buffer layers in this three-layer PHJ were the same as those in the Y6//PM6 PHJ, indicating that the field-dependent charge generation in the PHJ did not come from the buffer layers.

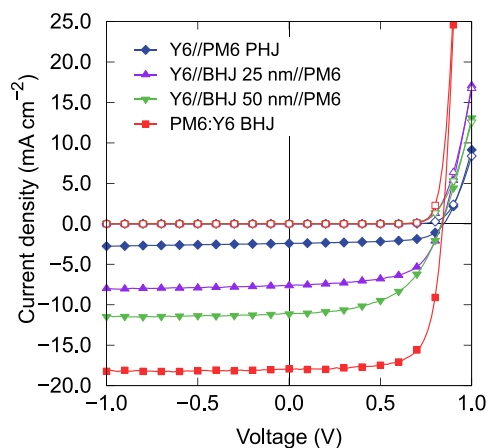
In addition, we examined the effect of an intentionally formed mixed interlayer between the donor and acceptor pure domains on the charge generation. We fabricated the three-layered PHJ structure using a film transfer technique (Figure S7) to mimic the interlayer in the PHJ structure. We inserted a thin BHJ layer of PM6:Y6 (1–2 nm) between the Y6 and PM6 layers in the PHJ structure as a pseudo interlayer at the D/A domain interface. We also fabricated the pseudo interlayer by molecular diffusion of Y6 into a thin (~ 1 nm) PM6 layer. J - V curves under light irradiation and normalized curves are shown in Figure S7b–e. The intentionally inserted pseudo interlayers barely affected the field-dependent charge generation. It is possible that the interlayer did not perfectly reproduce the interlayer in the actual BHJ layer; however, if the unintentional interlayer is the origin of the field-independent charge generation in the BHJ device, changes in the slope in J - V curves should be observed. This result suggests that other factors that have a greater effect on the field dependence of charge generation than the presence of the interlayer at the D/A interface.

(a)

MoO ₃ /Ag
PM6 ~ 45 nm
PM6:Y6 BHJ x nm
Y6 ~ 55 nm
ITO/PFN-Br

The BHJ layer and PM6 layer were sequentially stacked onto the Y6 layer by a film transfer method.

(b)



(c)

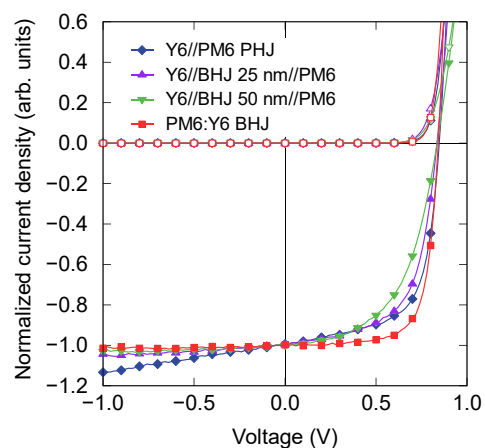


Figure S6 | (a) Device structure of the three-layered devices, in which the PM6:Y6 BHJ layer is inserted between the Y6 and PM6 layers in the PHJ. The thickness of the BHJ layer was 25 or 50 nm. (b) J - V characteristics under AM1.5 100 mW/cm² irradiation. (c) Normalized J - V curve.

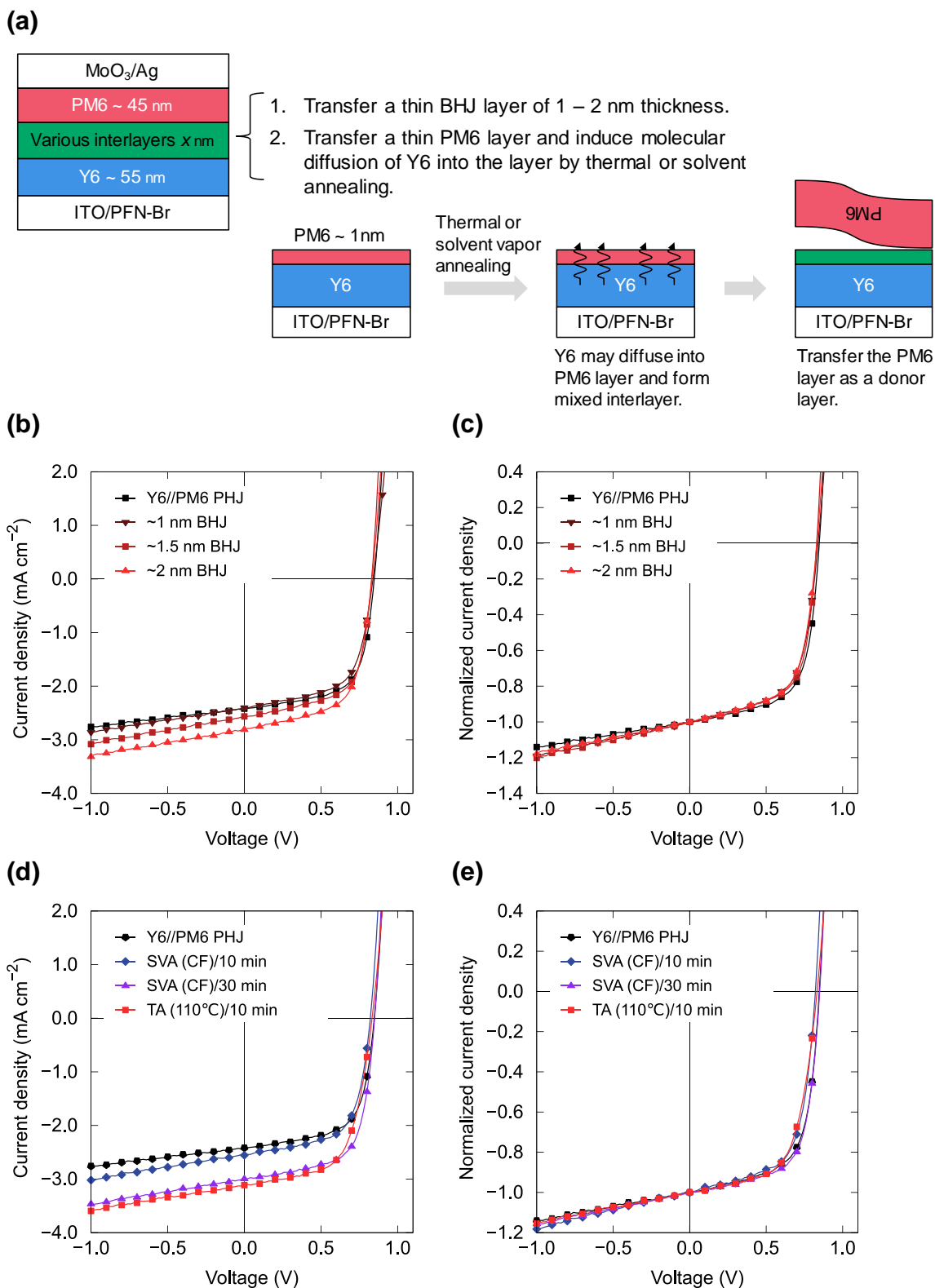


Figure S7 | (a) Device structure and fabrication procedure of the three-layered devices. For the devices with the BHJ interlayer, a very thin PM6:Y6 BHJ film was transferred onto the Y6 acceptor layer. The PM6 donor layer was transferred onto the BHJ layer, forming the three-layered structure. For the molecularly diffused interlayer, a very thin PM6 layer (~1 nm) was transferred onto the Y6 acceptor layer. Then, this two-layered structure was thermally annealed (TA) at 110 °C or solvent vapor

annealed (SVA) with chloroform (CF) for 10 and 30 min. This annealing induced molecular diffusion of Y6 into the thin PM6 layer. Finally, the donor PM6 layer was transferred. (b) J - V characteristics of the three-layered devices containing the inserted BHJ under AM1.5 100 mW/cm² irradiation. That of the Y6//PM6 PHJ device is shown for comparison. (c) Normalized J - V curve corresponding to the J - V curve in (b). (d) J - V characteristics of the three-layered devices with a molecularly diffused interlayer under AM1.5 100 mW/cm² irradiation. (e) Normalized J - V corresponding to the J - V curve in (d).

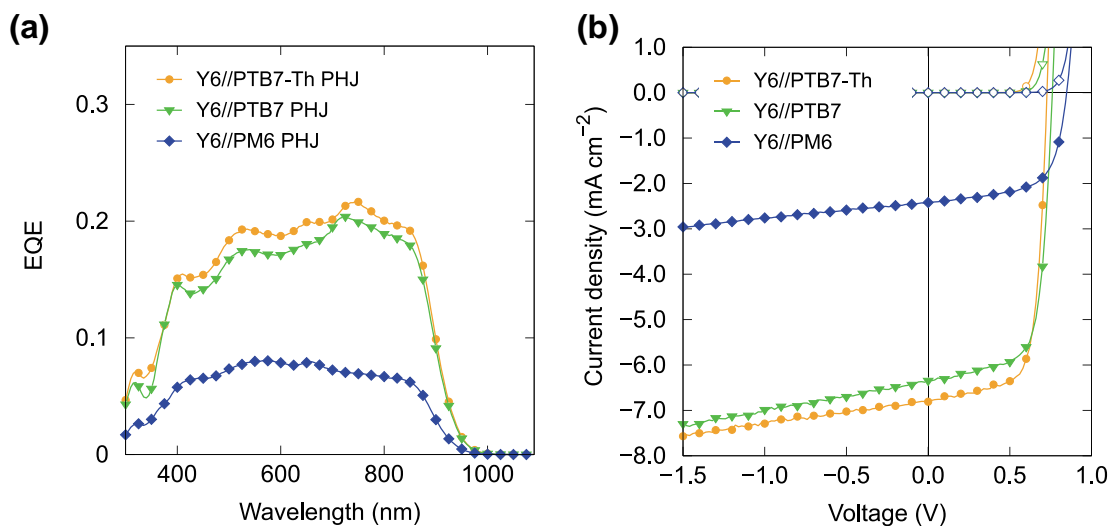


Figure S8 | EQE and J - V curves of Y6//PTB7-Th, Y6//PTB7 and Y6//PM6 PHJ devices. (a) EQE and (b) J - V characteristics under AM1.5 100 mW/cm² light irradiation.

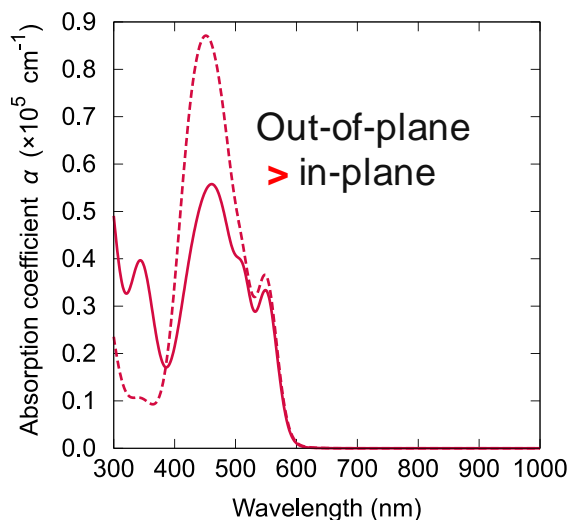
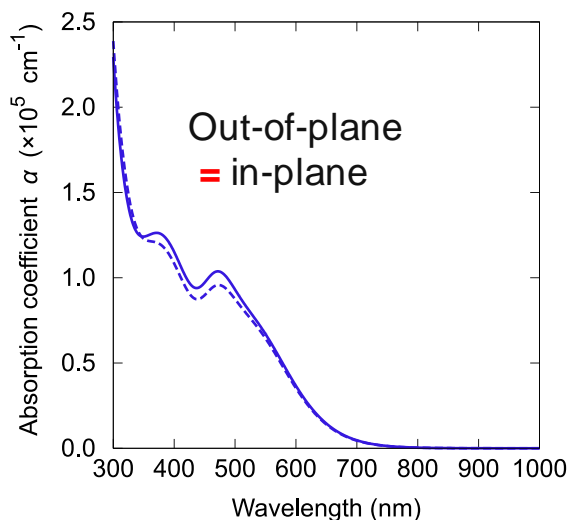
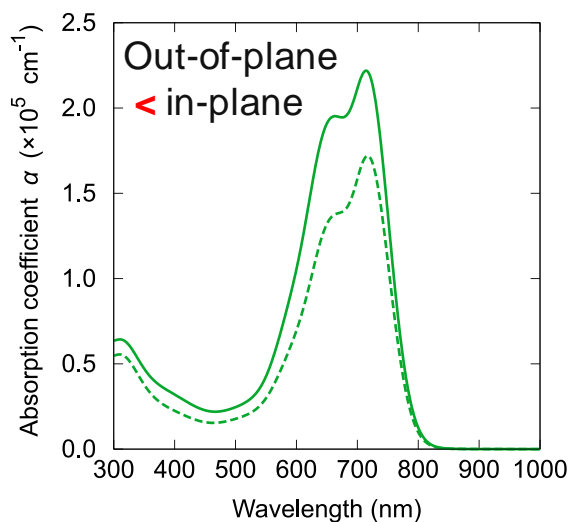
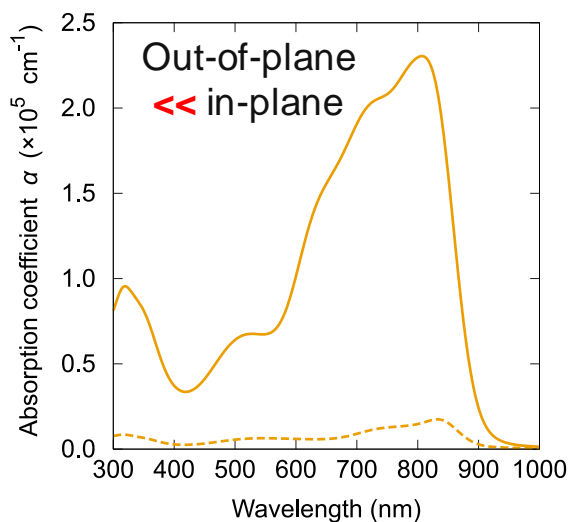
(a) PhC₂-BQQDI**(b) PC₇₁BM****(c) IT-4F****(d) Y6**

Figure S9 | Optical anisotropy in the in-plane and out-of-plane directions determined by variable-angle spectroscopic ellipsometry. The solid and dashed lines are the absorption coefficients in the in-plane and out-of-plane directions, respectively. (a) PhC₂-BQQDI, (b) PC₇₁BM, (c) IT-4F, and (d) Y6 pristine films.

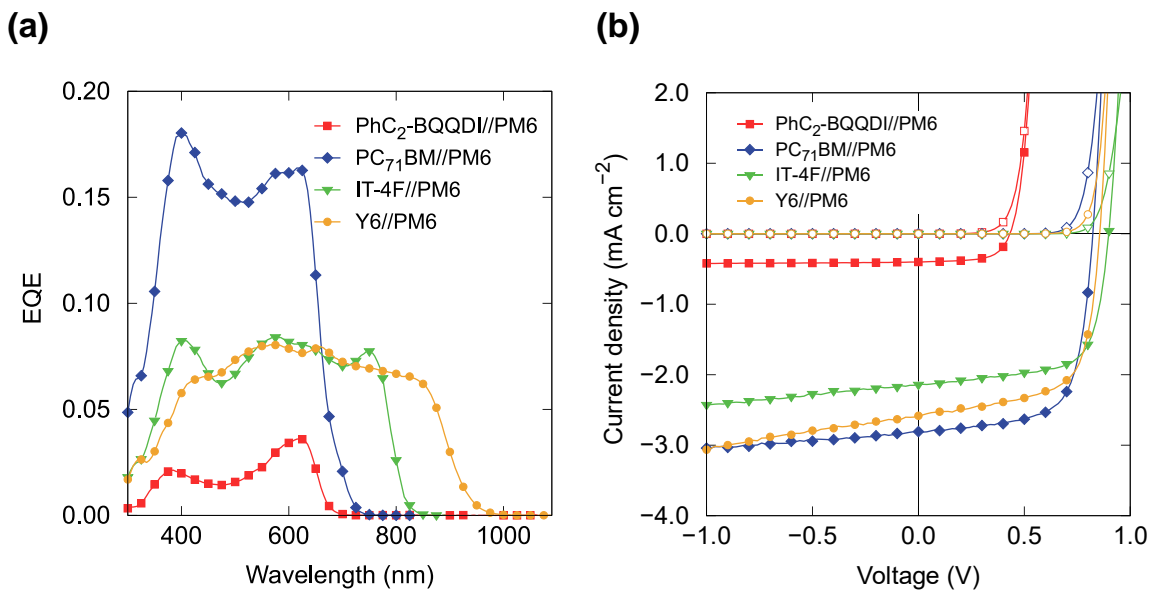


Figure S10 | EQE and $J-V$ curves of PhC₂-BQQDI//PM6, PC₇₁BM//PM6, IT-4F//PM6, and Y6//PM6 PHJ devices. (a) EQE and (b) $J-V$ characteristics under AM1.5 100 mW/cm² light irradiation.

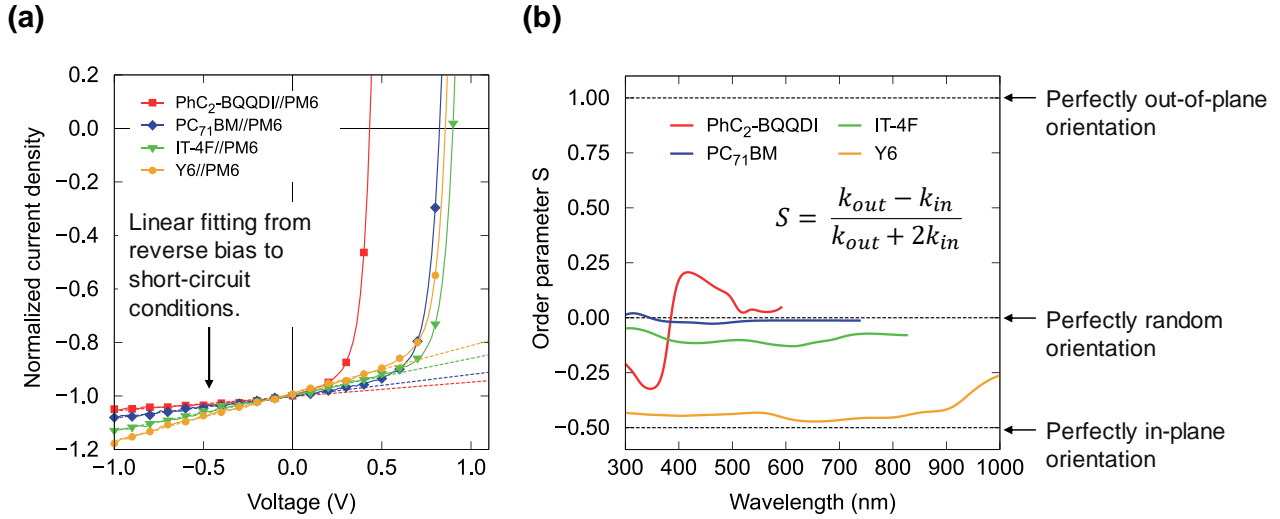


Figure S11 | Calculation of the slope in the J - V curve and order parameter S . (a) Slope value extracted by linear fitting to the J - V curve from reverse bias to short-circuit conditions extracts. (b) Order parameter S of the acceptor pristine films. S was calculated using anisotropic extinction coefficients in the in-plane (k_{in}) and out-of-plane (k_{out}) directions. S values of 1.0, 0, and -0.5 indicate perfectly out-of-plane, random, and in-plane orientations.

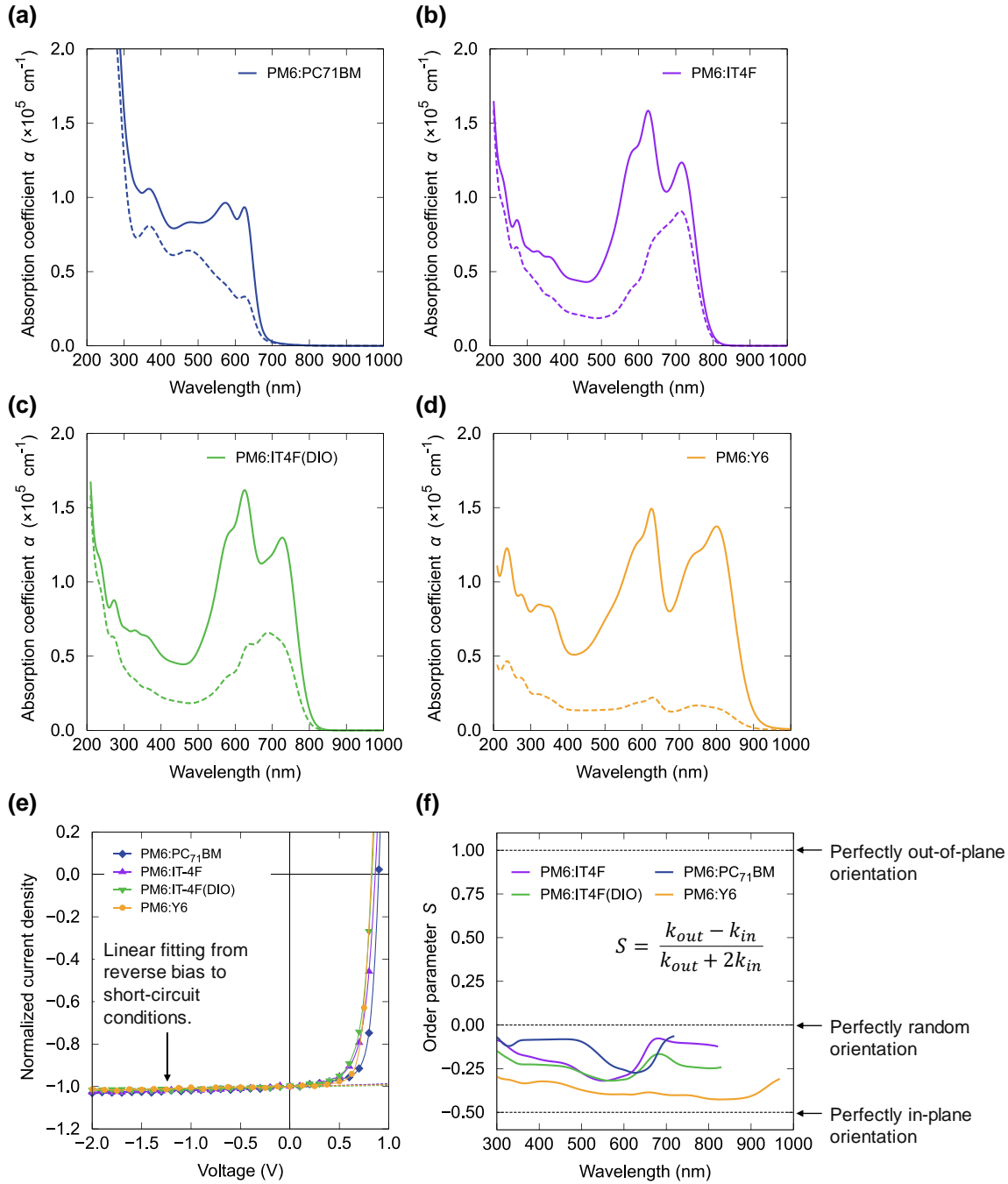


Figure S12 | Optical anisotropy in the in-plane and out-of-plane directions determined by variable-angle spectroscopic ellipsometry. The solid and dashed lines are the absorption coefficients in the in-plane and out-of-plane directions, respectively. (a) PM6:PC₇₁BM BHJ film, (b) PM6:IT-4F BHJ film, (c) PM6:IT-4F BHJ film with DIO additive, and (d) PM6:Y6 BHJ film. (e) Slope value extracted by linear fitting to the J - V curve from reverse bias to short-circuit conditions. (f) Order parameter S of the BHJ films. S was calculated using anisotropic extinction coefficients in the in-plane (k_{in}) and out-of-plane (k_{out}) directions at the peak-top wavelength of the acceptor. S values of 1.0, 0, and -0.5 indicate perfectly out-of-plane, random, and in-plane orientations.

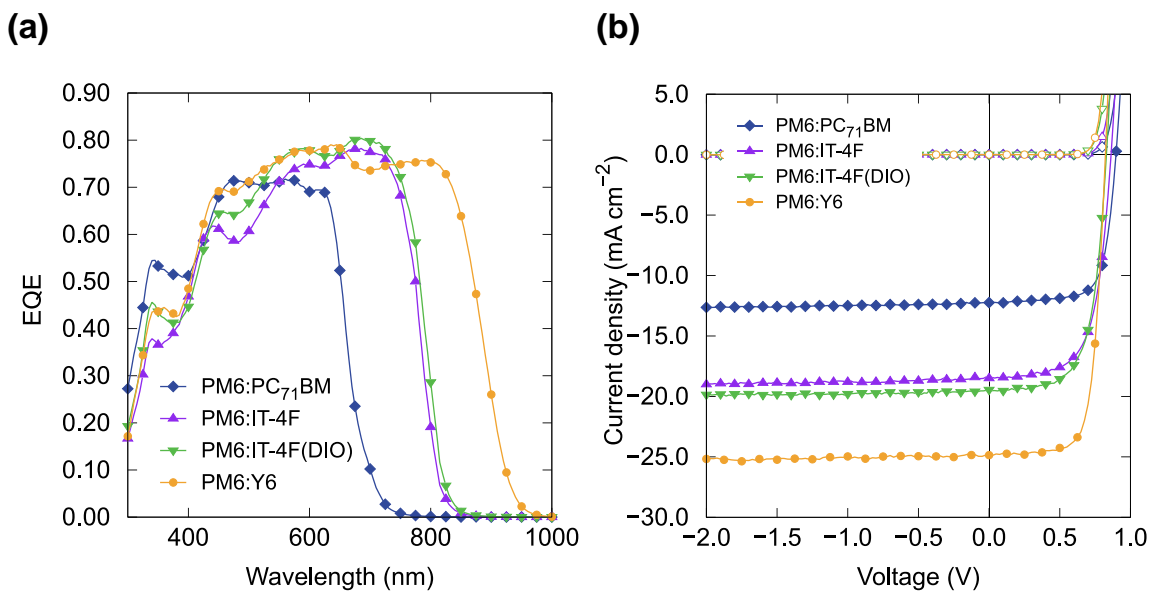


Figure S13 | EQE and J - V curves of PM6:PC₇₁BM, PM6:IT-4F, PM6:IT-4F with DIO, and PM6:Y6 BHJ devices. (a) EQE and (b) J - V characteristics under AM1.5 100 mW/cm² light irradiation.

Table S3. Summary of short-circuit current (J_{SC}), open-circuit voltage (V_{OC}), fill factor (FF), and power conversion efficiency (PCE) values. Donor material is PM6 for all devices. Numbers in parentheses are standard deviations calculated from at least six devices.

Acceptor	Structure	J_{SC} (mA cm ⁻²)	V_{OC} (V)	FF	PCE (%)
PhC ₂ -BQQDI	PHJ	-0.38 (0.022)	0.42 (5.9×10^{-3})	0.62 (0.004)	0.10 (0.007)
PC ₇₁ BM	PHJ	-2.87 (0.049)	0.83 (4.9×10^{-3})	0.67 (0.014)	1.59 (0.013)
	BHJ	-12.16 (0.11)	0.91 (1.5×10^{-2})	0.71 (0.029)	7.9 (0.25)
IT-4F	PHJ	-2.11 (0.022)	0.89 (4.7×10^{-3})	0.69 (0.005)	1.30 (0.019)
	BHJ	-18.08 (0.38)	0.88 (1.5×10^{-2})	0.67 (0.023)	10.51 (0.41)
	BHJ w/DIO	-19.53 (0.12)	0.83 (1.7×10^{-3})	0.66 (0.010)	10.72 (0.15)
Y6	PHJ	-2.46 (0.11)	0.85 (4.7×10^{-3})	0.64 (0.013)	1.34 (0.069)
	BHJ	-24.35 (0.70)	0.85 (0.016)	0.74 (0.015)	15.22 (0.36)